Am J Transl Res 2024;16(5):1602-1619
www.ajtr.org /ISSN:1943-8141/AJTR0156373

Original Article

Cepharanthine inhibits migration, invasion, and EMT of bladder cancer cells by activating the Rap1 signaling pathway in vitro

Bo Chen[1,2], Lin Chen[1,2], Jin Yang[1,2], Mingqiang Hou[3], Qibo Cai[3], Wenbin Dai[1,2], Xin Zhou[1,2], Weiwei Wang[1,2], Xiaoming Long[4], Na Yin[5]

[1]Department of Urology, Zunyi Medical University, Zunyi 563000, Guizhou, China; [2]Department of Urology, Clinical Medical College and Affiliated Hospital of Chengdu University, Chengdu 610000, Sichuan, China; [3]Department of Urology, Xishui County People's Hospital, Zunyi 563000, Guizhou, China; [4]Department of Pharmacy, Clinical Medical College and Affiliated Hospital of Chengdu University, Chengdu 610000, Sichuan, China; [5]Department of Urology, The Third Affiliated Hospital of Zunyi Medical University, Zunyi 563000, Guizhou, China

Received March 5, 2024; Accepted April 23, 2024; Epub May 15, 2024; Published May 30, 2024

Abstract: Background: Cepharanthine, a bioactive constituent of *Stephania japonica* (*Thunb.*) *Miers,* is known for its potent anti-tumor properties. Nevertheless, the precise impact of this substance on bladder cancer remains poorly comprehended. The aim of this study was to demonstrate the effect and mechanism of cepharanthine on the metastasis of human bladder cancer cells. Methods: The application of network pharmacology was utilized to ascertain the possible targets and signaling pathways of cepharanthine in the treatment of bladder cancer. The antiproliferative effects of cepharanthine were evaluated using Cell Counting Kit-8 and colony formation assays. The migration and invasion capabilities were assessed using Transwell assays and wound healing experiments. Proteins related to the Rap1 signaling pathway, cellular migration, cellular invasion, and Epithelial-Mesenchymal Transition (EMT) were quantified by western blotting. Results: Through database screening, 313 cepharanthine-acting targets, 277 candidate disease targets in bladder cancer, 22 intersecting targets, and 12 core targets were confirmed. The involvement of the Rap1 signaling system was revealed by the Kyoto Encyclopedia of Genes and Genomes' pathway enrichment study. Cepharanthine was shown to decrease bladder cancer cell proliferation, migration, and invasion *in vitro*. Cepharanthine activated the Rap1 signaling pathway by upregulating Epac1 and downregulating E-cadherin and C3G protein expression, leading to increased expression of Rap1 GTP protein and decreased expression of protein kinase D1 and integrin α5. Rap1 signalling pathway activation resulted in the downregulation of migration and invasion-related proteins, matrix metallopeptidase MMP2, MMP9, as well as EMT-related proteins, N-cadherin and Snail, without affecting vimentin expression. Conclusion: Cepharanthine inhibits migration, invasion, and EMT of bladder cancer cells by activating the Rap1 signalling pathway. The results offer helpful insights regarding the possible therapeutic use of cepharanthine for treating bladder cancer.

Keywords: Cepharanthine, bladder cancer, network pharmacology, Rap1 signaling pathway, cell migration, cell invasion

Introduction

Bladder cancer is a prevalent tumor worldwide, with uroepithelial cancer as its main histological type [1]. The prevalence and fatality rates of bladder cancer are notably higher in men compared to women, which have consistently remained increased since the year 2020 [2]. Bladder cancer is classified into two types: non-muscle invasive bladder cancer (NMIBC) and muscle-invasive bladder cancer (MIBC). NMIBC comprises roughly 75% of newly diagnosed cases, while the remaining cases are MIBC, characterized by deeper infiltration into the bladder wall or metastasis [3].

Current treatment options for bladder cancer include transurethral resection of the bladder tumor (TURBT), radical cystectomy, radiotherapy, chemotherapy, immunotherapy, and targeted therapy [4]. TURBT and adjuvant Bacillus Calmette-Guérin vaccine therapy are commonly

https://doi.org/10.62347/WDFF7432

used for NMIBC, but their clinical benefits are limited [5, 6]. Radical treatment is primary for MIBC; however, it often leads to impairments in urinary, bowel, and sexual functions, significantly impacting patients' quality of life [7-9].

Tumor metastasis involves a dynamic multistep process of cell migration and invasion, regulated by intrinsic and extrinsic factors [10]. The Rap1 signaling pathway, crucial for cell adhesion, integration, and invasive behaviors, is implicated in bladder cancer metastasis [11]. Network pharmacology, a modern approach that combines systems biology and computational analysis, is utilized in our study to predict the targets and signaling pathways of cepharanthine in bladder cancer, offering a holistic view of the drug's multifaceted effects on cellular processes and its potential mechanisms in inhibiting tumor metastasis.

Traditional Chinese medicine (TCM) plays a significant role in bladder cancer therapy, with increasing focus on understanding its effects and mechanisms of action. Several studies have explored TCM treatments for bladder cancer, such as using artesunate, baicalin, and Xiaozheng Decoction [12-14]. *Stephania japonica (Thunb.) Miers*, a TCM herb known for its heat-clearing and detoxifying properties, has been extensively documented and is specifically effective for urinary urgency, pain, discomfort, and swelling. Cepharanthine, an active component extracted from *Stephania japonica (Thunb.) Miers*, has a variety of biological activities such as anti-inflammatory, antiviral, antitumor and anti-organ fibrosis effects [15-21]. Despite some focus on cepharanthine's role in drug resistance, there is limited literature on its effects on bladder cancer, particularly regarding migration and invasion. Furthermore, the specific targets and molecular processes of cepharanthine have yet to be determined [22-24].

Hence, this research employed network pharmacology to predict the targets and signalling pathways of cepharanthine for the purpose of treating bladder cancer. Additionally, we investigated the molecular mechanisms of cepharanthine and its impact on bladder cancer cell proliferation, migration, and invasion *in vitro*.

Materials and methods

Prediction of the drug targets and bladder cancer disease targets of cepharanthine

The molecular structure of cepharanthine was acquired from PubChem (https://pubchem.ncbi.nlm.nih.gov/). The drug targets of cepharanthine were obtained from the Swiss Target Prediction database (http://www.swisstargetprediction.ch/) and the Pharm Mapper database (http://www.lilab-ecust.cn/pharmmapper/submitfile.html), while the gene symbols were obtained from the Uniprot database (https://www.uniprot.org/). The drug targets from both databases were merged based on gene symbols, resulting in the identification of drug targets for cepharanthine after elimination of any duplicate targets. The disease targets for bladder cancer in Homo sapiens were obtained from the GeneCards database (https://www.genecards.org/), and candidate disease targets with relevant score ≥ 30.0 were chosen.

Analysis of the overlapping targets and construction of a network of protein-protein interactions (PPI) between cepharanthine and bladder cancer

The drug targets of cepharanthine and the candidate disease targets in bladder cancer were crossed using the Venny 2.1.0 database (https://bioinfogp.cnb.csic.es/tools/venny/index.html) to obtain potential therapeutic targets for bladder cancer treatment with cepharanthine. The potential targets were then imported into the STRING database (https://cn.string-db.org/) for construction of a PPI network, which was visualized using Cytoscape 3.9.0. The top 10 key targets in terms of degree and MCC values were filtered using the Cytohubba plugin, and the intersection of both values was considered as the core target of cepharanthine for treating bladder cancer.

Gene ontology and Kyoto Encyclopedia of Genes and Genomes signaling pathway enrichment analysis

The prospective therapeutic targets derived from the overlap of the drug and disease targets were imported into the DAVID database (https://david.ncifcrf.gov/) for GO functional annotation and KEGG pathway enrichment

analysis. The Microbiology Letter online data analysis and visualization website (http://www.bioinformatics.com.cn/) was used to present graphical representations of the top 10 count values for biological process (BP), cellular components (CC), and molecular function (MF) in GO functional annotation, as well as the top 20 count values for KEGG pathway enrichment. The significance level was established at a *P*-value of less than 0.05. Additionally, KEGG enrichment analysis was conducted on the core targets. The resultant signaling pathways were then compared to those obtained for the possible therapeutic targets to validate the identified pathways.

Cepharanthine-bladder cancer-target-pathway network construction

The cepharanthine-bladder cancer-target-pathway network map was visualized using Cytoscape 3.9.0, which included cepharanthine, bladder cancer, the potential therapeutic targets obtained by intersecting cepharanthine and bladder cancer, and the top 20 pathways obtained from KEGG enrichment analysis.

Cell culture

The G2 and G3 cell lines, 5637 and HT1376 respectively, are representative of different grades in bladder cancer. These cell lines were acquired from Wuhan Shangen Biotechnology in China. They were cultivated in Roswell Park Memorial Institute-1640 medium supplemented with 10% FBS from Dayou in China, along with 1% antibiotic containing 100 U/mL penicillin G and 100 μg/mL streptomycin. The subculture process was initiated when the cell confluence reached 80%. Subsequently, the cells were cultured under specific conditions, maintaining a temperature of 37°C, a carbon dioxide concentration of 5%, and a humidity level ranging from 70% to 80%.

Cell proliferation assay

Cepharantine was procured from MedChemExpress, with a purity ≥ 99.71% and catalog number HY-N6972. HT1376 and 5637 cells were inoculated onto 96-well plates at a density of 5000 cells per well. Following cell attachment, the cells were subjected to treatment with different concentrations (0, 5, 10, 15, 20, 25, and 30 μM) of cepharanthine (dissolved in dimethyl sulfoxide) for 24 h, resulting in a final dimethyl sulfoxide concentration of 2.5/1000 (v/v) in the drug sample. Following PBS washing, the wells were treated with CCK-8 reagent (APExBIO, USA) and incubated at 37°C in full media for 2 h. The measurement of absorbance at 450 nM was conducted using the Thermo Fisher Scientific Varioskan LUX multipurpose enzyme marker (Thermo Fisher, China). Cell viability (%) was calculated as [(absorbance of cepharanthine-treated group - absorbance of blank control group)/(absorbance of untreated cells group - absorbance of blank control group)] ×100%.

Colony formation assay

Six-well plates were seeded with 1000 HT1376 and 5637 cells, dispersed evenly. The cells were treated with 0, 10, or 20 μM of cepharanthine for 24 h. Subsequently, fresh medium was introduced, and the cells were placed in an incubator for 10 days. After incubation, the cells were washed with PBS and fixed with 4% paraformaldehyde for 1 h before being stained with 0.1% crystalline violet (Solarbio, China) for 30 min. The staining solution was removed using running water, and the cells were observed and photographed after drying. The cells were scanned using a microscope slide scanner NanoZoomer S360 (Hamamatsu Photonics, Japan), and the colonies were counted using Image J software.

Wound healing assay

HT1376 and 5637 cells were seeded at an appropriate density in six well plates. Once the cells covered the entire culture dish after attachment, they were starved for 12 h in a serum-free medium. The cells were then treated with 0, 10, or 20 μM of cepharanthine after being scratched with a 200 μL gun tip and cleaned with PBS. Migration was observed and documented using an inverted fluorescence microscope (Olympus IX73, Japan). Cell migration was quantitatively analyzed using the Image J software.

Transwell cell migration assay

HT1376 and 5637 cells were seeded into six-well plates at a density of 2×10^5 cells per well. Following attachment, the cells were exposed to 0, 10, or 20 μM of cepharanthine for 24 h.

Subsequently, the cells were collected and reconstituted in a medium devoid of serum, with the cell density modified to 3×10^5/mL. In the lower transwell chamber, 600 μL of complete medium containing 20% FBS was added, while in the upper chamber, 200 μL of cell suspension treated with medicines was added. After 24 h of cell development, the cells were immobilized by exposure to a 4% paraformaldehyde solution for 30 min. Afterwards, 0.1% crystal violet dye (Solarbio, China) was applied to the cells for another 30 min. After being washed with PBS, the cells and crystal violet staining solution were carefully removed from the bottom of the upper chamber using a damp cotton swab. Afterwards, the samples were thoroughly dried and viewed using a fluorescence microscope for observation and quantification. The cells were observed and recorded using an inverted fluorescent microscope (Olympus IX73, Japan), and the analysis was performed using Image J software.

Transwell cell invasion assay

HT1376 and 5637 cells were seeded in 6-well plates at a density of 2×10^5 cells per well. Following attachment, the cells were exposed to 0, 10, or 20 μM of cepharanthine for 24 h. The cells were harvested in a medium without serum, and the density of cells was adjusted to 3×10^5 cells/mL. The matrix gel was composed of BD Matrigel and serum-free medium in a ratio of 1:8, which had been pre-cooled to 4°C. Subsequently, 600 μL of complete medium including 20% fetal bovine serum (FBS) was introduced into the lower transwell chamber, while the upper chamber was filled with 200 μL of medication-treated cell suspension. The cells were incubated for 24 h, fixed with 4% paraformaldehyde for 30 min to maintain their structure, and then stained with a 0.1% crystal violet solution (Solarbio, China) for 30 min. Following PBS washing, the cells and crystal violet staining solution were carefully removed from the bottom of the upper chamber using a damp cotton swab. Subsequently, the cells were adequately air-dried and captured using a fluorescence microscope (Olympus IX73, Japan) for observation and quantified using Image J software.

Western blot

Following the optimum seeding density of HT1376 and 5637 cells into 6-well plates, the cells were exposed to 0, 10, and 20 μM cepharanthine for 24 h, and then rinsed with PBS. 200 μl of lysis solution with protease inhibitor (Solarbio, China) was added to each well, and the lysis process was carried out on ice for 20 min. Subsequently, the lysate was collected, subjected to centrifugation, and the resulting liquid above the sediment was obtained by aspiration. The protein concentration was standardized to 1 mg/ml using a BCA Protein Quantification Kit (Thermo Fisher, China). For sodium dodecyl sulphate (SDS)-polyacrylamide gel electrophoresis, we employed 10-30 μg of total protein samples. The separation gel concentration was set at 8-12%. After separation, the proteins were transported to polyvinylidene difluoride membranes (Millipore, USA), which were subsequently blocked with 5% skimmed milk powder for 1 h at room temperature. Then, they were incubated overnight at 4°C with primary antibodies against GAPDH (HuaBio; Cat: ET1601-4; 1:8000), Rap1 (Cell Signaling Technology; Cat: 2399S; 1:500), Epac1 (HuaBio; Cat: ET1705-79; 1:1000), E-cadherin (Cell Signaling Technology; Cat: 3195S; 1:1000), C3G (Santa Cruz; Cat: sc-17840; 1:1000), PKD1 (HuaBio; Cat: ET1705-4; 1:1000), ITGA5 (HuaBio; Cat: ET1610-15; 1:1000), MMP2 (Abcam; Cat: ab97779; 1:1000), MMP9 (Cell Signaling Technology; Cat: 13667T; 1:1000), N-cadherin (HuaBio; Cat: M1304-1; 1:1000), Snail (HuaBio; Cat: ER1706-22; 1:1000), and Vimentin (Santa Cruz; Cat: sc-6260; 1:1000). After a thorough cleaning with TBST solution three times (5 min for each), the membranes were exposed to secondary antibodies for 1 h at ambient temperature, followed with TBST rinse again for three times (10 min for each). Protein visualization was carried out using the ChemiDoc XRS+ system in conjunction with the ECL (Abbkine, Wuhan, China) developer. The grayscale intensity of all protein bands was determined using Image J software, with GAPDH serving as the reference for loading normalization. The ultimate outcomes were represented as the grayscale value of the target band divided by the grayscale value of GAPDH.

Active Rap1 detection

The active form of the Rap1 protein was identified in cellular lysates using an active Rap1 pull down and detection kit provided by Cell Signaling Technology. HT1376 and 5637 cells

were seeded onto 6-well plates at suitable cell densities, exposed to 0, 10, and 20 μM of cepharanthine for 24 h, and then rinsed with PBS. A lysis buffer solution containing phenylmethylsulfonyl fluoride was applied for 5 min, and the cell debris were removed by using centrifugal force. Subsequently, the liquid portion of the mixture was used for BCA protein measurement and the creation of a lysate with a concentration of 1 mg/ml. The sample, bound protein, and glutathione resin were mixed in a rotating cup and kept at a temperature of 4°C for 1 h. This allowed the GTP-bound GTPase to attach to the glutathione resin via the GST-linked binding protein. The protein that was not bound was separated by centrifugation, while the GTPase that was attached to the glutathione resin was released using SDS buffer containing dithiothreitol (DTT) with a final concentration of 200 mM. The eluted samples were subjected to western blot analysis to quantify the quantity of active Rap1 protein.

Quantitative data analysis

The statistical analysis was conducted with IBM SPSS Statistics 27.0.1 software. The data were collected from three separate and repeated studies, and the findings were presented as the mean value ± the standard deviation (SD). Independent samples t-tests were used to test for significant differences between two groups of data; one-way ANOVA was used to analyze significant differences between three or more groups, with statistical significance defined at P-value < 0.05.

Results

Molecular structure of cepharanthine and its potential therapeutic targets in bladder cancer treatment

The chemical configuration of cepharanthine was acquired from PubChem and graphically shown using ChemDraw 21.0.0 (**Figure 1A**). In order to determine the possible therapeutic targets of cepharanthine for the treatment of bladder cancer, the Swiss Target Prediction and Pharm Mapper databases were utilized, and yielded a compilation of drug action targets linked to cepharanthine, resulting in a total of 313 relevant targets. Additionally, we retrieved information on bladder cancer disease targets from the GeenCards database, which yielded a total of 9,291 targets. By setting the relevance score threshold to ≥c30.0, we identified 277 candidate disease targets specifically related to bladder cancer. To determine the potential therapeutic targets of cepharanthine for bladder cancer treatment, we performed an intersection analysis between the drug action targets and the bladder cancer disease targets. Through Venn plots (**Figure 1B**), we obtained a total of 22 intersecting targets, suggesting that these targets may play a role in the treatment of bladder cancer with cepharanthine and have the potential to be targeted for therapeutic purposes.

Construction of a PPI network map and core target screening

A PPI network diagram was created to explore possible therapeutic targets of cepharanthine for the treatment of bladder cancer, as shown in **Figure 1C**. The CytoHubba plugin was utilized to select the Degree Top10 and MCC Top10 core targets, as displayed in **Figure 1D**. The Degree Top10 core targets included EGFR, MET, MTOR, FGFR1, TERT, SRC, JAK2, ESR1, MDM2, and AKT1, while the MCC Top10 core targets consisted of ESR1, TERT, MDM2, SRC, EGFR, MET, KIT, FGFR1, ALK, and MTOR. A total of 12 non-repeating core targets were identified, highlighted in **Figure 1E**.

GO study of putative cepharanthine medicinal targets for bladder cancer therapy

Figure 1F shows the findings of GO functional annotation analysis for putative therapeutic targets of cepharanthine for bladder cancer therapy. In BP, 91 enriched GO terms were identified, with a focus on signal transduction, protein autophosphorylation, and negative regulation of apoptosis. 21 enriched GO items were detected in CC, predominantly associated with the plasma membrane, nucleus, and cytosol. In MF, 34 enriched GO terms were identified, mainly involving protein binding, identical protein binding, and adenosine triphosphate binding.

KEGG pathway enrichment study of potential cepharanthine medicinal targets for bladder cancer therapy

Figure 1G displays the results of KEGG pathway enrichment analysis for the potential therapeu-

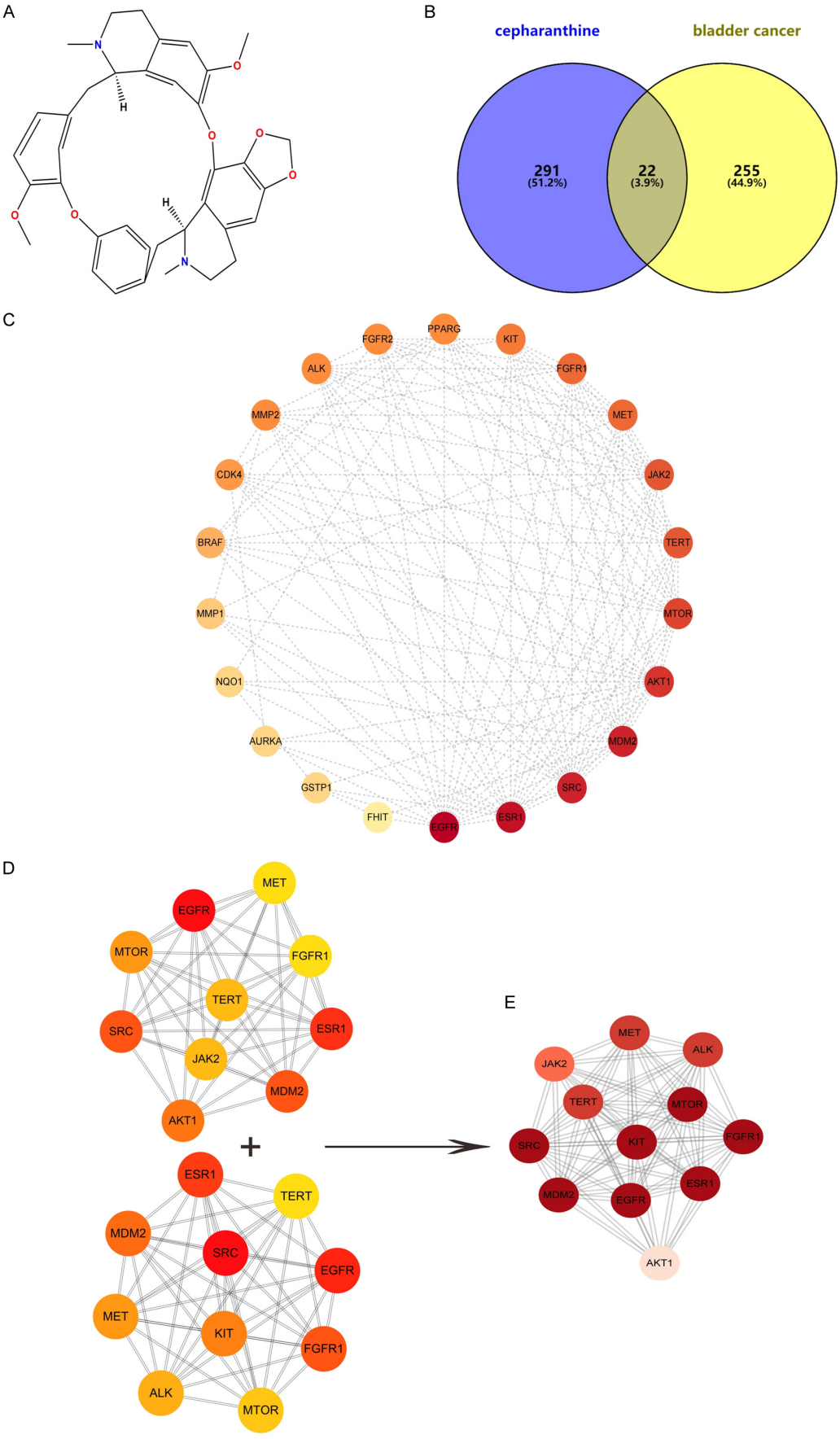
A
B
cepharanthine
bladder cancer
291
(51.2%)
22
(3.9%)
255
(44.9%)
C
PPARG
KIT
FGFR1
MET
JAK2
TERT
MTOR
AKT1
MDM2
SRC
ESR1
EGFR
FHIT
GSTP1
AURKA
NQO1
MMP1
BRAF
CDK4
MMP2
ALK
FGFR2
D
MET
EGFR
MTOR
FGFR1
TERT
SRC
ESR1
JAK2
MDM2
AKT1
ESR1
TERT
MDM2
SRC
EGFR
MET
KIT
FGFR1
ALK
MTOR
E
MET
ALK
JAK2
TERT
MTOR
SRC
KIT
FGFR1
MDM2
EGFR
ESR1
AKT1

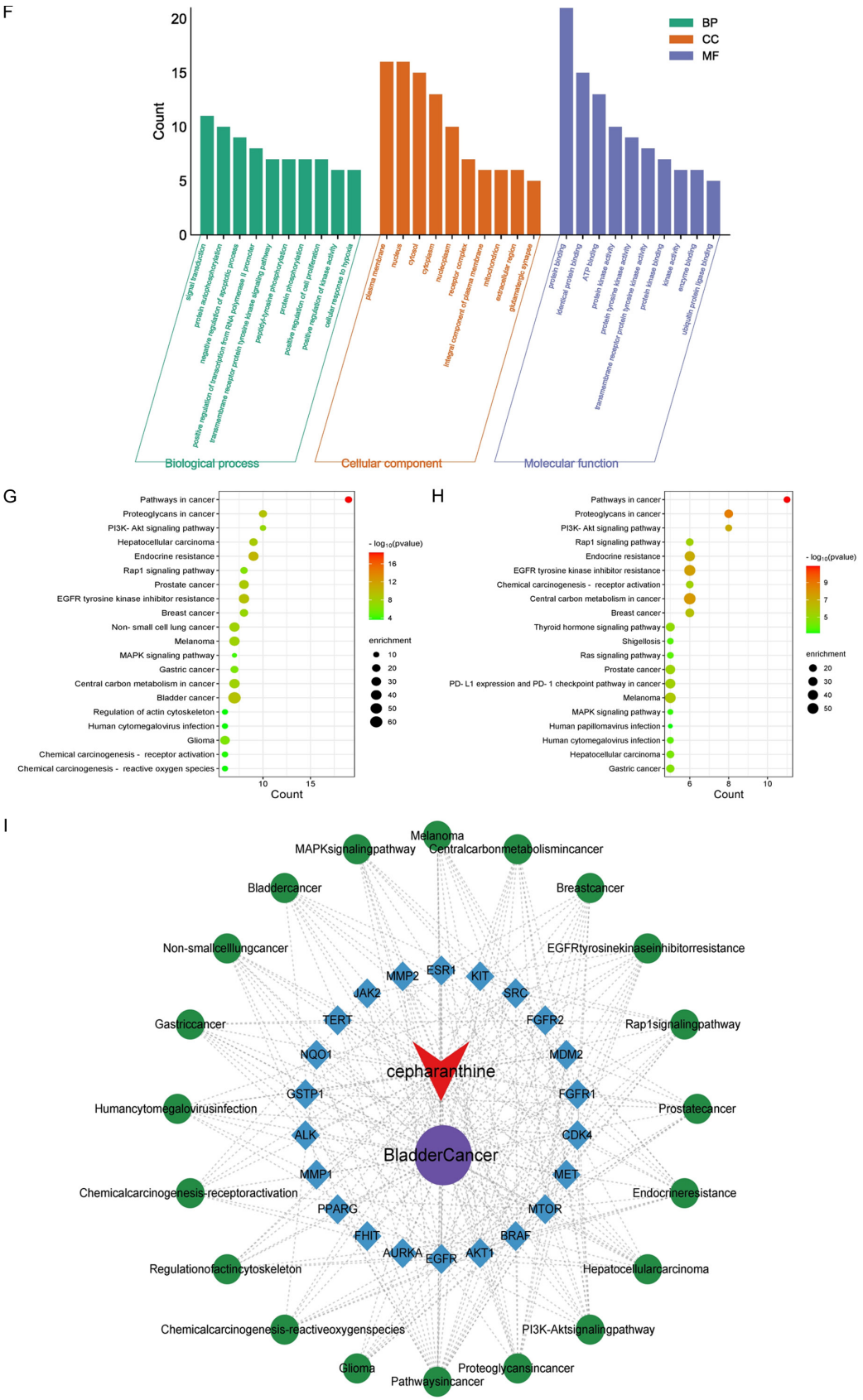
F
BP
CC
MF
Count
Biological process
Cellular component
Molecular function
G
Count
H
Count
I
cepharanthine
BladderCancer

Figure 1. Molecular structure of cepharanthine, potential therapeutic targets of cepharanthine on bladder cancer, PPI network visualization, core targets, GO, KEGG enrichment analysis, and drug-disease-target-pathway visualization of cepharanthine. A. Molecular structure of cepharanthine. B. Overlapping cepharanthine-related and bladder cancer-related targets on Venn diagram. C. Visualization of PPI network of potential therapeutic targets. D. Top 10 ranking of Degree and MCC values. E. Twelve core targets from the intersection of Degree Top10 and MCC Top10. F. GO enrichment analysis. The top 10 functional categories of biological processes, cellular components, and molecular functions were selected for display. G. KEGG pathway enrichment analysis of the potential therapeutic targets. The 20 pathways with the highest count values were selected for display. H. Results of KEGG pathway enrichment analysis of core targets. I. Visual network diagram of drug-disease-target-pathway of cepharanthine for bladder cancer treatment.

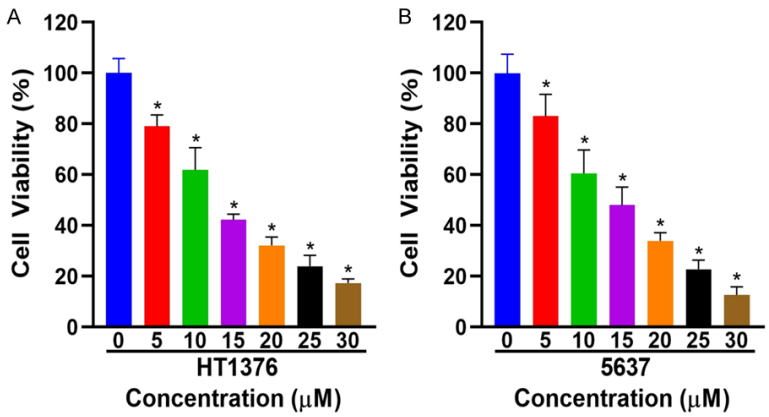

Figure 2. Inhibitory effects of cepharanthine on the viability of bladder cancer cells. Cell viability of HT1376 (A) and 5637 (B) bladder cancer cells treated with different concentrations of cepharanthine for 24 h, was detected by the CCK-8 method. Values are expressed as mean ± SD, $n = 3$ (experiments were repeated in triplicate independently), $^{*}P < 0.05$ *vs.* control group (concentration: 0 μM).

tic targets of cepharanthine in the treatment of bladder cancer. Enrichment analysis identified that potential targets were implicated in 76 signaling pathways, with prominent pathways encompassing cancer, proteoglycans in cancer, the PI3K-Akt signaling pathway, hepatocellular carcinoma, endocrine resistance, the Rap1 signaling pathway, prostate cancer, EGFR tyrosine kinase inhibitor resistance, and breast cancer. These findings indicate that cepharanthine may exert its anti-bladder cancer actions via many signaling pathways.

Results of drug-disease-target-pathway analysis

A drug-disease-target-pathway network diagram was created to visualize the potential interactions among cepharanthine, bladder cancer, therapeutic targets, and pathways, as shown in **Figure 1I**. The analysis demonstrated that cepharanthine has multi-target and multi-pathway interactions, suggesting its potential efficacy as an anti-bladder cancer agent.

Cepharanthine inhibited the vitality of bladder cancer cells

The impact of cepharanthine on the viability of bladder cancer cells was assessed by CCK-8 test after 24 h of treatment with different doses (0, 5, 10, 15, 20, 25, and 30 μM). Following cepharanthine treatment, the cell viability of HT1376 and 5637 cells dropped considerably. HT1376 cell viability reduced significantly from 100% to (17.36 ± 1.56)% ($P < 0.05$) (**Figure 2A**), while 5637 cell viability declined significantly from 100% to (12.65 ± 3.25)% ($P < 0.05$) (**Figure 2B**). The IC_{50} values of cepharanthine in HT1376 and 5637 cells were determined to be 11.18 and 11.58 μM, respectively.

Cepharanthine inhibited bladder cancer cell proliferation in vitro

To assess the impact of cepharanthine on the proliferation of bladder cancer cells, we conducted a colony formation test using the HT1376 and 5637 cell lines. As demonstrated in **Figure 3**, the clonogenic numbers of bladder cancer cells decreased gradually as the concentrations of cepharanthine increased, indicative of a concentration-dependent inhibition of cell proliferation.

Cepharanthine reduced migration, invasion, and EMT of bladder cancer cells

To examine the potential inhibitory effects of cepharanthine on the migration, invasion, and EMT of bladder cancer cells, we performed wound healing, transwell migration and inva-

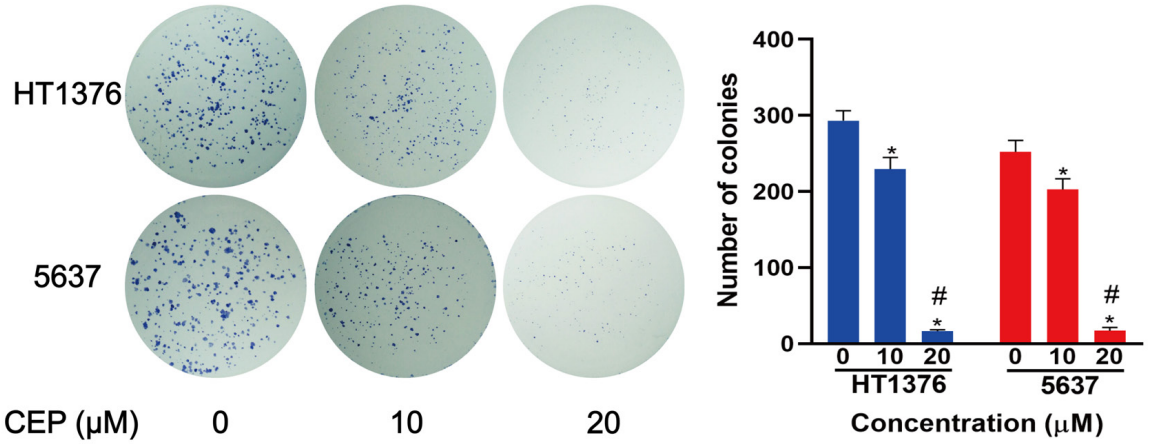

Figure 3. Effect of cepharanthine on colony forming ability of HT1376 and 5637 cells. Cells were treated with cepharanthine and then cultured in fresh medium for 10 days to form colonies. Values are expressed as mean ± SD, n = 3 (experiments were repeated in triplicate independently), $^{*}P < 0.05$ *vs.* untreated group (concentration: 0 μM), $^{\#}P < 0.05$ *vs.* treatment group (concentration: 10 μM). Note: CEP: cepharanthine.

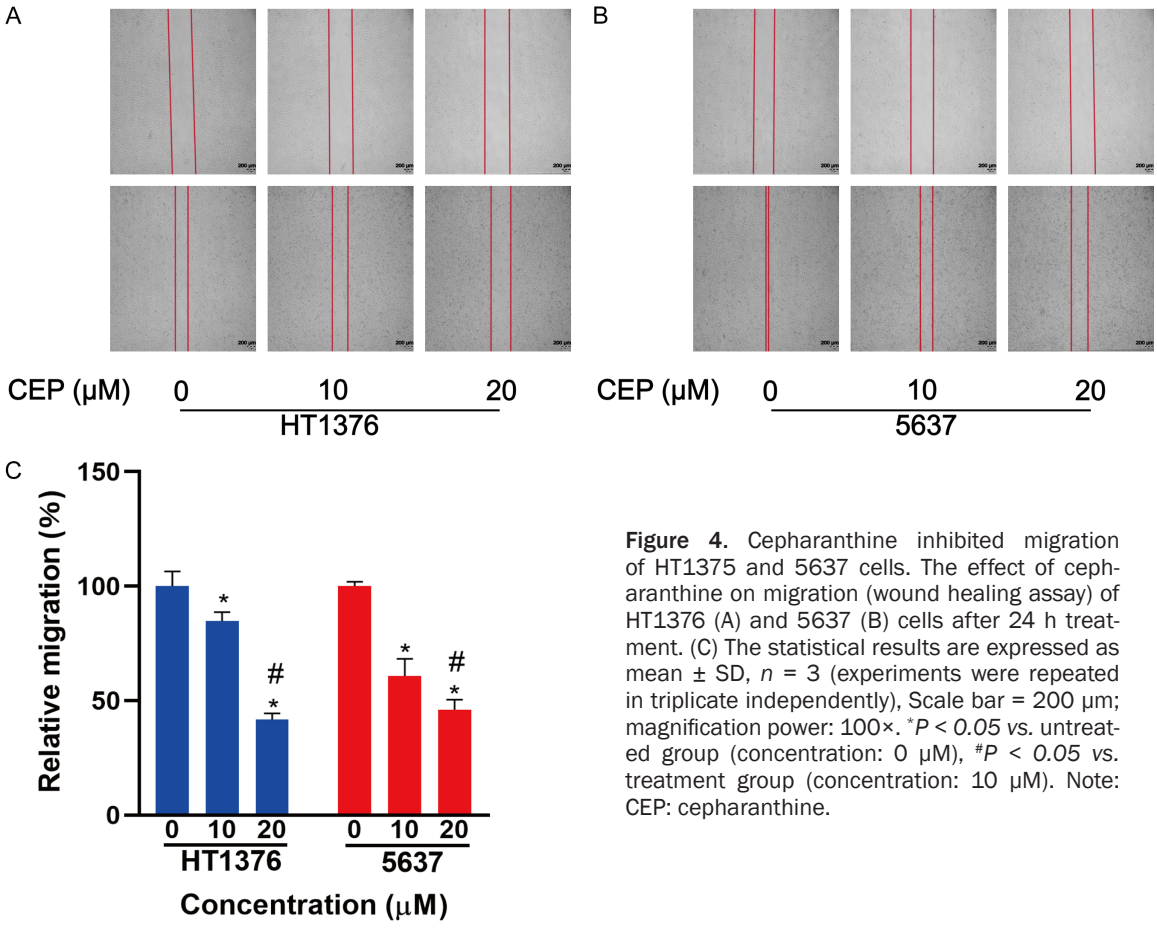

Figure 4. Cepharanthine inhibited migration of HT1375 and 5637 cells. The effect of cepharanthine on migration (wound healing assay) of HT1376 (A) and 5637 (B) cells after 24 h treatment. (C) The statistical results are expressed as mean ± SD, n = 3 (experiments were repeated in triplicate independently), Scale bar = 200 μm; magnification power: 100×. $^{*}P < 0.05$ *vs.* untreated group (concentration: 0 μM), $^{\#}P < 0.05$ *vs.* treatment group (concentration: 10 μM). Note: CEP: cepharanthine.

sion assays using HT1376 and 5637 cell lines. After 24 h, the wound area in untreated control group was considerably larger compared to that in the cepharanthine-treated group (10 μM, 20 μM), as seen in **Figure 4**. Furthermore, the transwell migration and

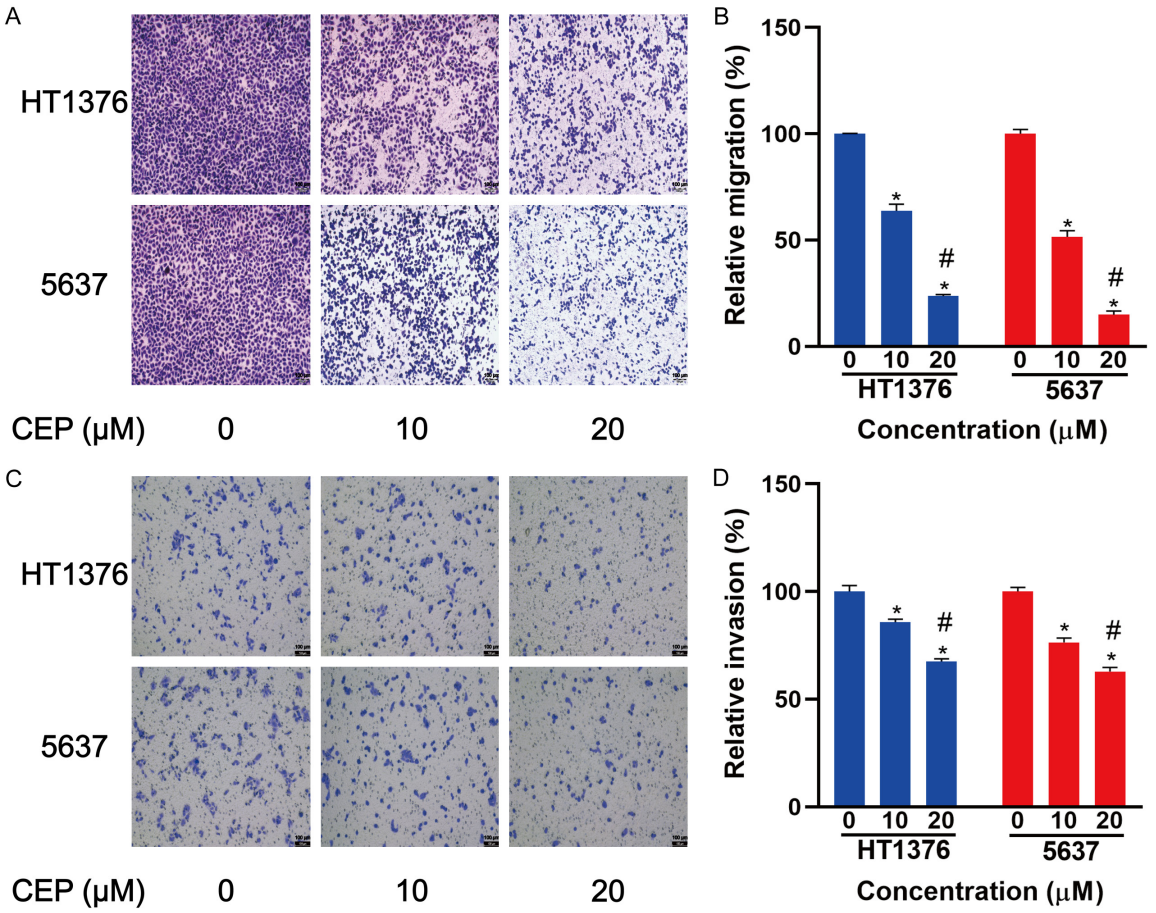

Figure 5. The effect of cepharanthine on migration and invasion (transwell assay) of HT1376 and 5637 cells after 24 h treatment. Migration (A, B) and invasion (C, D) abilities were observed by transwell assay. Values are expressed as mean ± SD, $n = 3$ (experiments were repeated in triplicate independently), Scale bar = 100 μm; magnification power: 200×. $^{*}P < 0.05$ *vs.* untreated group (concentration: 0 μM), $^{\#}P < 0.05$ *vs.* treatment group (concentration: 10 μM). Note: CEP: cepharanthine.

invasion assays revealed a significant decrease in the rate of cell perforation in the treated groups as compared to the control group (**Figure 5**). In addition, the western blotting study showed a reduction in the expression of MMP2, MMP9, N-cadherin, and Snail. However, the levels of Vimentin didn't change greatly (**Figure 6A-D**). These data indicate that cepharanthine can suppress the migration, invasion, and EMT process of bladder cancer cells.

Activation of Rap1 signaling pathway by cepharanthine

Based on the KEGG enrichment analysis of drug-disease crossover targets, the Rap1 signaling pathway was identified as a potential pathway involved in the therapeutic effects of cepharanthine on bladder cancer. To validate this hypothesis, we performed a KEGG enrichment analysis (**Figure 1H**) of the previously obtained drug-disease core targets, which confirmed the involvement of the Rap1 signaling pathway. Additionally, we evaluated the activation of the Rap1/PKD1/ITGA5 pathway (**Figure 7**) and observed that the expression of active Rap1 protein was upregulated with increasing drug concentrations, while the downstream protein molecules PKD1 and ITGA5 were downregulated (**Figure 8**). Furthermore, western blotting analysis indicated a dose-dependent decrease in E-cad/C3G expression and an increase in Epac1 expression after the administration of cepharanthine, providing insight into its mechanism of action through the Rap1 signaling pathway.

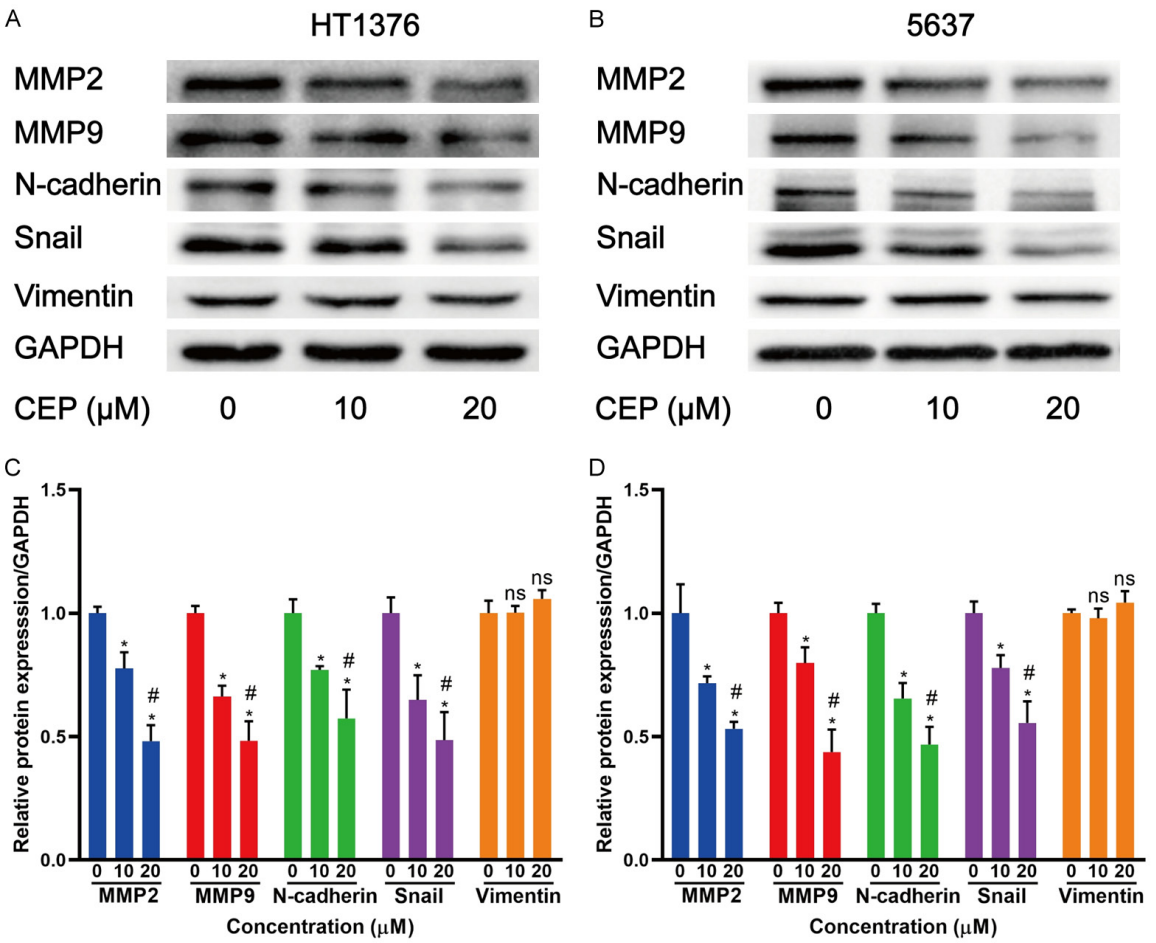

Figure 6. Cepharanthine inhibited the expression of migration and invasion related proteins in HT1376 and 5637 cells. The effect of cepharanthine on the expression levels of migration and invasion related proteins MMP2, MMP9, and EMT-related proteins, detected by western blotting, in HT1376 (A, C) and 5637 (B, D) cells after 24 h treatment. Values are expressed as mean ± SD, $n = 3$ (experiments were repeated in triplicate independently), $^{*}P < 0.05$ *vs.* untreated group (concentration: 0 μM), $^{\#}P < 0.05$ *vs.* treatment group (concentration: 10 μM). Note: CEP: cepharanthine; MMP2: matrix metalloproteinase 2; MMP9: matrix metalloproteinase 9; EMT: epithelial-mesenchymal transition.

Discussion

Bladder cancer is a highly prevalent and deadly tumor, ranking among the top 10 most common cancers worldwide [2]. The metastasis rate of bladder cancer is also alarmingly high [25]. Despite advancements in treatment, patients with metastatic bladder cancer still face significant challenges, including low 5-year survival rates [26]. Hence, it is essential to investigate novel therapeutic agents and techniques for the treatment of bladder cancer, particularly in tackling the problem of metastasis. Cepharanthine, an active compound found in the plant *Stephania japonica (Thunb.) Miers* [15], has shown promise in influencing various biological behaviors of tumors, such as cell proliferation [18], apoptosis [19, 27], migration, and invasion [28]. Furthermore, recent research has shown its capacity to hinder the multiplication of viruses, suggesting its promise as a therapy for severe acute respiratory syndrome caused by coronavirus 2 [17]. As understanding of cepharanthine grows, researchers have begun investigating its antitumor and antiviral effects. However, there is a lack of exploratory studies specifically examining its anti-bladder cancer effects and underlying mechanisms. Our research used network pharmacology and *in vitro* experiments to investigate the anti-bladder cancer properties of cepharanthine. We have identified possible targets and the

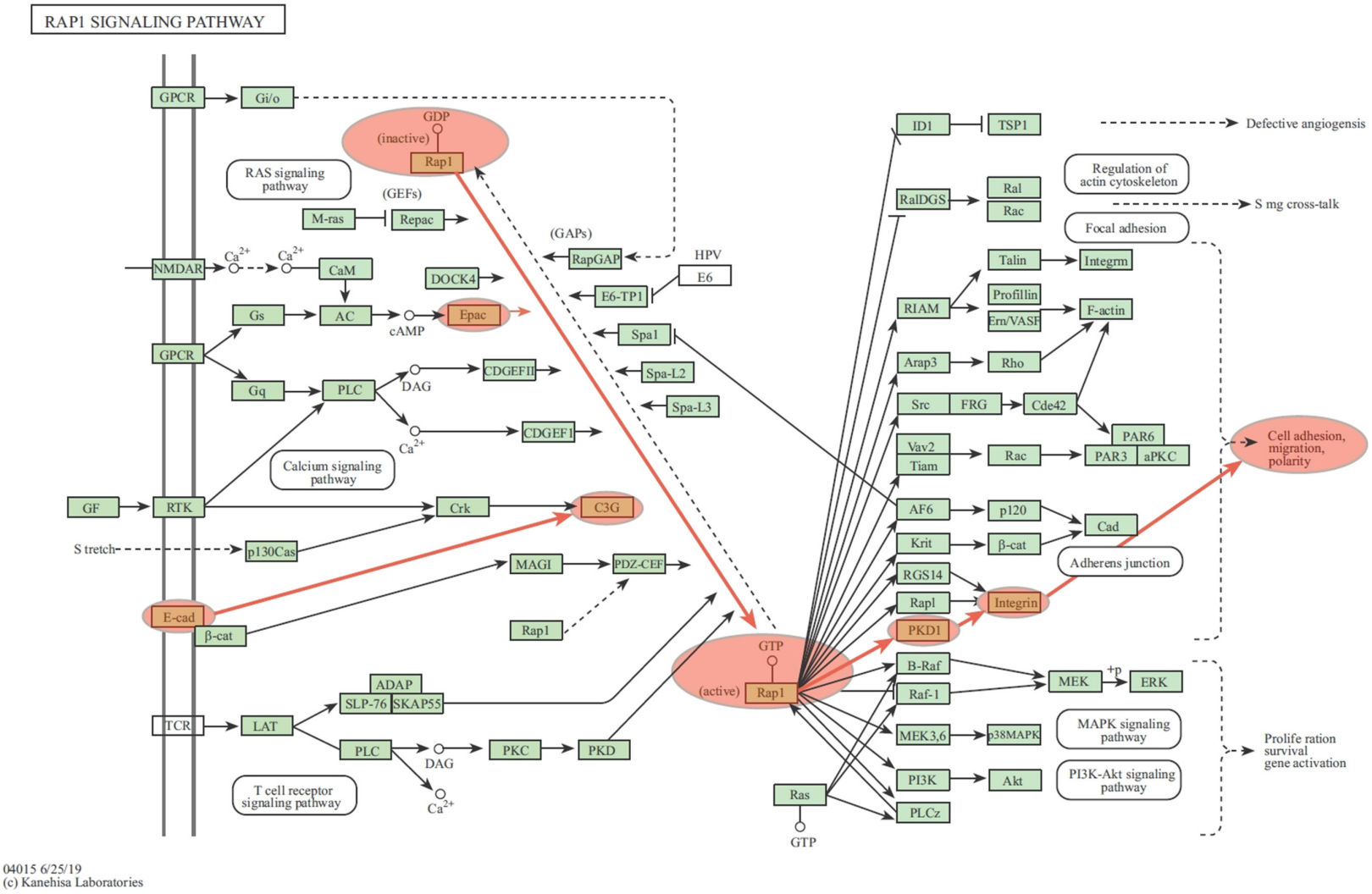

Figure 7. Rap1 signaling pathway. The highlighted part is the related pathway we focused on.

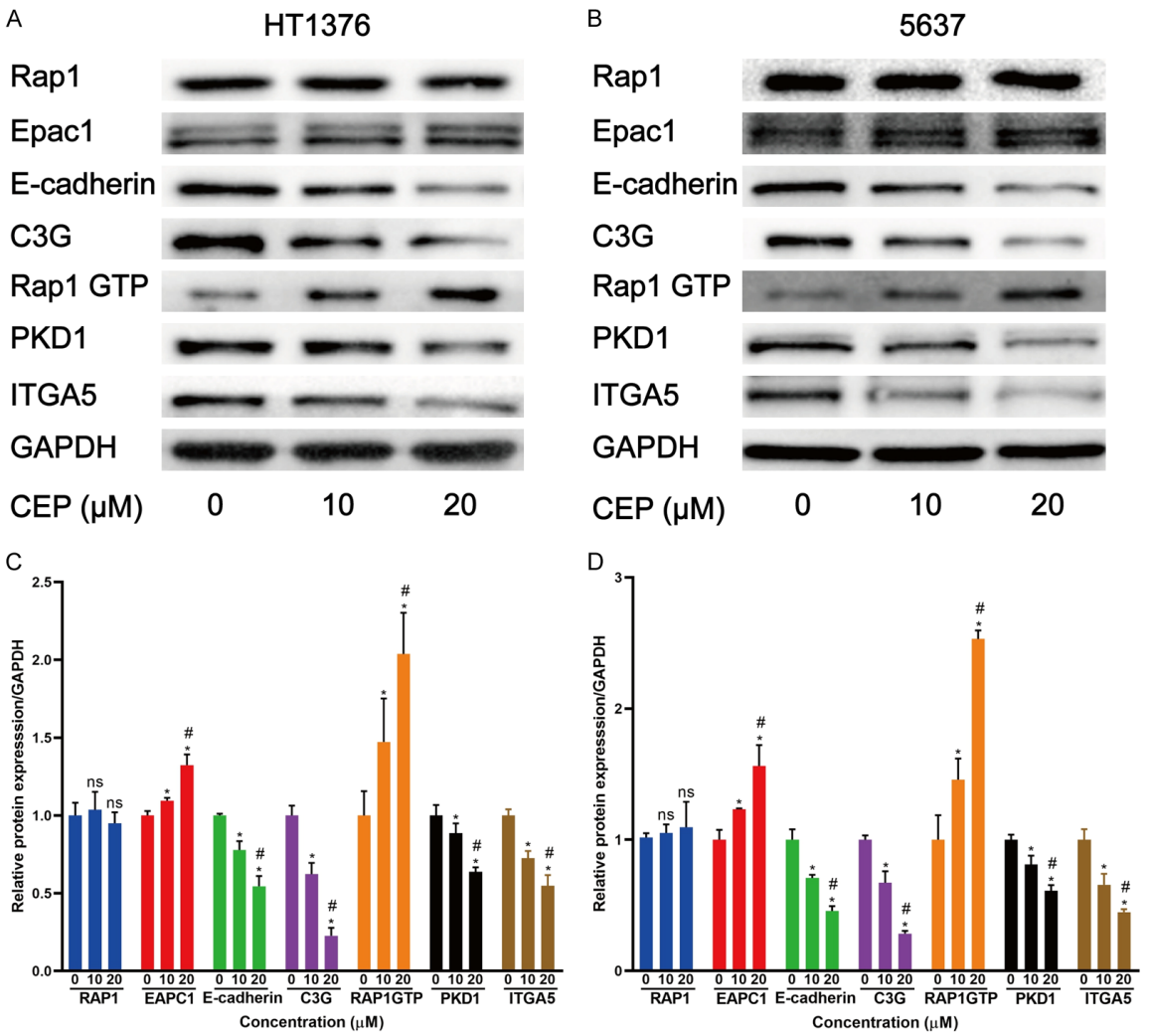

Figure 8. Cepharanthine activate Rap1 and affect the expression of related signaling pathway molecules. The effect of cepharanthine on the expression levels of Rap1, Epac1, E-cadherin, C3G, Rap1 GTP, PKD1, ITGA5, detected by western blotting, in HT1376 (A, C) and 5637 (B, D) cells after 24 h treatment. Values are expressed as mean ± SD, $n = 3$ (experiments were repeated in triplicate independently), $^{*}P < 0.05$ *vs.* untreated group (concentration: 0 μM), $^{\#}P < 0.05$ *vs.* treatment group (concentration: 10 μM). Note: CEP: cepharanthine; Rap1: Ras-proximate-1; Epac1: Exchange protein directly activated by cAMP 1; E-cadherin: epithelial cadherin; C3G: Crk SH3-domain-binding guanine-nucleotide-releasing factor; PKD1: protein kinase D1; ITGA5: integrin alpha-5.

molecular pathways involved. The specific flowchart is shown in **Figure 9**. TCM has garnered substantial recognition in disease treatment, leading to a surge in research efforts to explore its possible uses. We used internet databases and performed network pharmacology studies to thoroughly investigate the specific targets and mechanisms of action of cepharanthine in the treatment of bladder cancer. Subsequently, we conducted *in vitro* experiments to validate our findings. The KEGG enrichment analysis showed that cepharanthine was linked to various signaling pathways, such as cancer, proteoglycans in cancer, PI3K-Akt signaling pathway, hepatocellular carcinoma, endocrine resistance, Rap1 signaling pathway, prostate cancer, EGFR tyrosine kinase inhibitor resistance, and breast cancer (**Figure 1G**). Rap1, a small GTPase belonging to the Ras family [29], exhibits its dual biological functions: first, it can reverse KRAS-induced cell morphological alterations [30], and second, its activation can promote the development of various cancers through multiple signaling pathways [31, 32]. The Rap1 signaling pathway plays a crucial role in regulating several cancers, particularly in integrin fam-

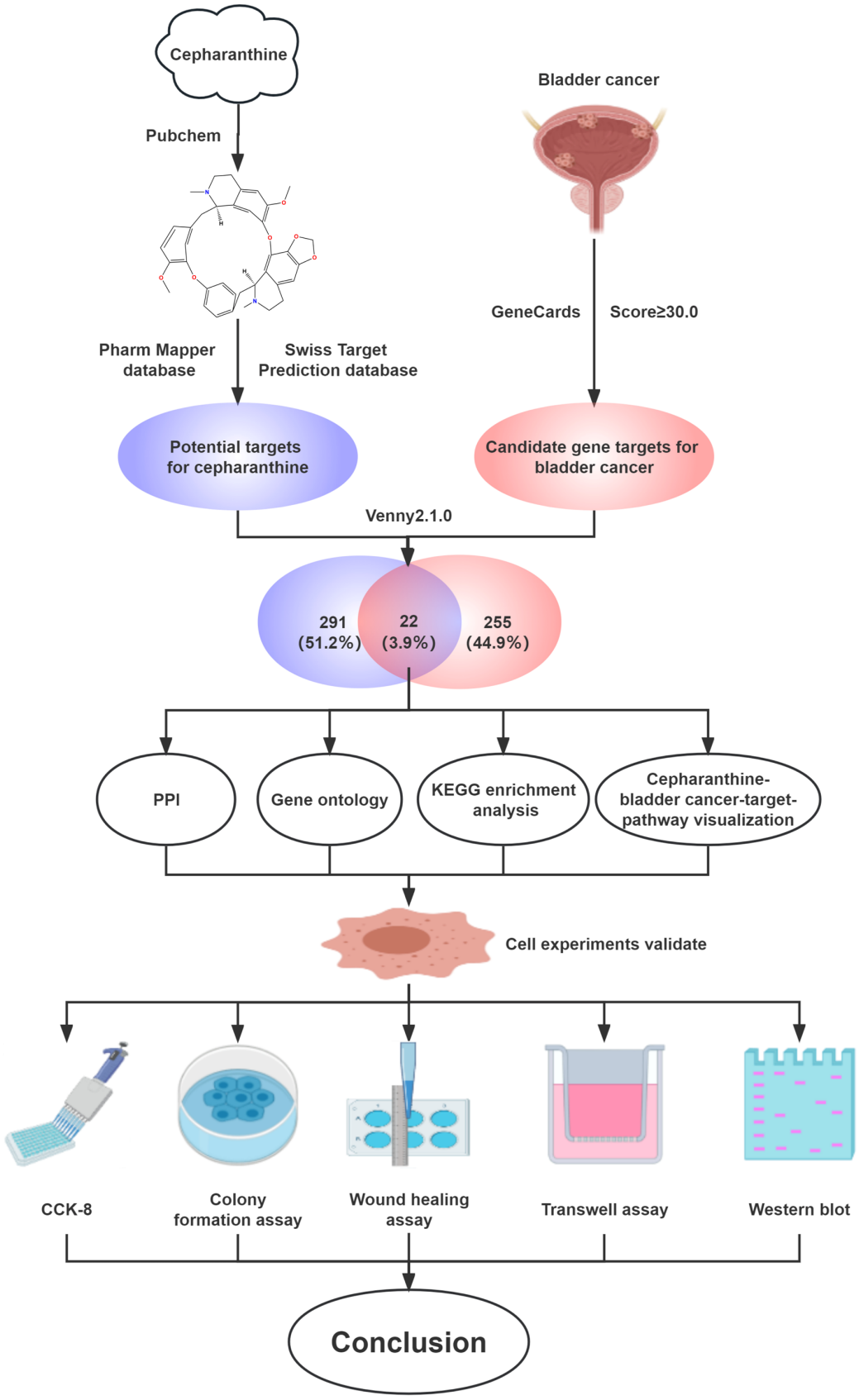

Figure 9. The flow chart for the network pharmacology analysis and *in vitro* validation.

ily-mediated processes such as cell adhesion, migration, and invasion [11]. Epac1, a guanylate exchange factor regulated by cyclic adenosine monophosphate (cAMP), is involved in GTP/GDP exchange and activation of the Rap1 signaling pathway for potential cancer therapeutic effects [33, 34]. C3G, another guanine nucleotide exchange factor (GEF) also known as RAPGEF1, plays an important role in the activation of the Rap1 signaling pathway [35]. PKD1, a member of the serine/threonine kinase family, functions as a significant controller in several biological processes such as cell migration, invasion, and EMT [36]. It is closely associated with the regulation of Rap1 and integrins [37, 38]. ITGA5, an integral part of the integrin family, plays a pivotal function in the invasion of cancer cells and is strongly linked to the process of metastasis [39]. In our study, we selected the bladder cancer cell lines 5637 (G2) and HT1376 (G3) for *in vitro* experiments. These cell lines represent intermediate to high-grade bladder cancers with relatively high metastatic potential [40]. We evaluated the effects of cepharanthine on bladder cancer cell migration, invasion, and the EMT process through the Rap1/PKD1/ITGA5 signaling pathway. The concentrations of cepharanthine used in subsequent drug experiments (10 μM, 20 μM) were determined based on the IC_{50} values observed in HT1376 and 5637 cells. The final concentration of dimethyl sulfoxide in the drug samples was 2.5/1000 (v/v), which has been reported to have little or no cytotoxicity under a concentration of 5/1000 (v/v) [41-43]. During additional experiments using colony formation, wound healing, transwell migration and invasion assays, we observed that cepharanthine effectively suppressed the proliferation, migration, and invasion of bladder cancer cells. Migration and invasion were chosen for comprehensive investigations of their molecular mechanisms. By network pharmacology analysis, our attention was directed towards the confirmation of the Rap1 signaling pathway.

Through western blotting, we observed that the Rap1 signaling pathway was activated, resulting in elevated Rap1 GTP manifestation in the bladder cancer cell lines HT1376 and 5637 after treatment with cepharanthine. Additionally, activated Rap1 suppressed the expression of PKD1 and ITGA5, and prevented MMP2, MMP9, N-cadherin, and snail expression. However, vimentin protein expression remained unaffected. To further investigate the regulatory mechanism of cepharanthine's action on Rap1 and confirm the expression level of Rap1 GTP, we examined the expression levels of Epac1, E-cadherin, and C3G, which are upstream molecules involved in the regulation of Rap1 activation, by using the technique of western blotting. Prior studies have shown an positive relationship between the expression levels of Rap1 GTP and the migratory and invasive capabilities of bladder cancer cells [35, 44]. We found that E-cadherin and C3G expressions were decreased, Epac1 expression was increased, and Rap1 GTP expression was increased after cepharanthine treatment. Our observation of Rap1 GTP expression disagrees with previous reports, suggesting that Epac1 overexpression in bladder cancer cells activates Rap1 and thus inhibits bladder cancer cell migration [45]. Lyle et al. also found that the activation of the Epac-Rap pathway by cAMP hinders the migration of epithelial cells [46]. In our western blot experiments, we noticed a double band for Epac1, which may be attributed to protein transcription and post-translational modifications generating multiple protein isoforms. We also observed downregulation of E-cadherin expression, an EMT-related protein, which differs from previous reports [47], indicating that downregulated E-cadherin inhibits bladder cancer metastasis. Furthermore, C3G expression was downregulated in our study, contradicting previously reported pro-migration and pro-EMT effects of downregulated C3G in other diseases [48]. It is possible that E-cadherin disengagement activates the Rap1 GTPase, and E-cadherin is mutually associated with the presence of C3G [49]. These results lead to the conclusion that cepharanthine hinders the migration and invasion of bladder cancer cells, as well as the process of EMT, via activating the Rap1 signaling pathway.

While our study provides significant insights into the therapeutic potential of cepharanthine in bladder cancer, it also comes with limitations. One of the main constraints is the reliance on *in vitro* experiments. Though these offer valuable information on cellular mechanisms, they cannot fully replicate the complexity of tumor behavior in the human body. Future research should, therefore, include *in vivo* stud-

ies to validate our findings in a more physiologically relevant context. Additionally, while network pharmacology has enabled us to predict and analyze the targets and pathways affected by cepharanthine, experimental validation of these targets in bladder cancer models remains crucial. Moreover, understanding the drug's pharmacokinetics and pharmacodynamics *in vivo* will be essential for translating these findings into clinical applications. Future studies should also explore the potential synergistic effects of cepharanthine with current bladder cancer treatments to enhance therapeutic efficacy and overcome drug resistance. Finally, considering the genetic and molecular heterogeneity of bladder cancer, investigating the effects of cepharanthine across different bladder cancer subtypes would provide deeper insights into its therapeutic potential and help personalize treatment strategies.

Conclusion

This study shows that cepharanthine has an impact on bladder cancer by influencing the Rap1 signaling pathway and regulating the expression of downstream proteins, such as PKD1 and ITGA5. Additionally, cepharanthine modulates the expression of proteins related to migration, invasion, and EMT. MMP2 and MMP9 are representative proteins involved in migration and invasion, while proteins such as E-cadherin, N-cadherin, and Snail are EMT-related proteins. These molecular alterations contribute to the suppression of bladder cancer cell motility, invasion, and EMT processes. Hence, cepharanthine exhibits potential as a viable therapeutic choice for the management of bladder cancer and the prevention of its metastases.

Acknowledgements

The present study was supported by the Natural Science Foundation from the Department of Science and Technology of Sichuan Province (grant No. 2022NSFSC1592), Research Projects from Chengdu Science and Technology (grant No. 2022-YF05-01441-SN), Sichuan Medical (Youth Innovative) Scientific Research Projects (grant Nos. Q23002, S22002, Q20013 and Q20013), Chengdu University Affiliated Hospital Climbing Talent Program, and the Innovation Team Project of Affiliated Hospital of Clinical School of Medicine of Chengdu University (CDFYCX202207), Teaching Reform Project of Chengdu University (grant Nos. cdjgb2022043, cdjgb2022166 and cdjgb2019005) and Program of Affiliated Hospital of Chengdu University (Nos. Y202204, Y202207).

Disclosure of conflict of interest

None.

Address correspondence to: Jin Yang and Lin Chen, Department of Urology, Zunyi Medical University, Campus 1 Road, Xinpu New District, Zunyi 563000, Guizhou, China. E-mail: yangjin@cdu.edu.cn (JY); linchen@cdu.edu.cn (LC)

References

[1] Lobo N, Afferi L, Moschini M, Mostafid H, Porten S, Psutka SP, Gupta S, Smith AB, Williams SB and Lotan Y. Epidemiology, screening, and prevention of bladder cancer. Eur Urol Oncol 2022; 5: 628-39.

[2] Sung H, Ferlay J, Siegel RL, Laversanne M, Soerjomataram I, Jemal A and Bray F. Global cancer statistics 2020: GLOBOCAN estimates of incidence and mortality worldwide for 36 cancers in 185 countries. CA Cancer J Clin 2021; 71: 209-49.

[3] Dobruch J and Oszczudłowski M. Bladder cancer: current challenges and future directions. Medicina (Kaunas) 2021; 57: 749.

[4] Lenis AT, Lec PM, Chamie K and Mshs MD. Bladder cancer: a review. JAMA 2020; 324: 1980-91.

[5] Symeonidis EN, Lo KL, Chui KL, Vakalopoulos I and Sountoulides P. En bloc resection of bladder tumors: challenges and unmet needs in 2022. Future Oncol 2022; 18: 2545-58.

[6] Valenza C, Antonarelli G, Giugliano F, Aurilio G, Verri E, Briganti A, Curigliano G and Necchi A. Emerging treatment landscape of non-muscle invasive bladder cancer. Expert Opin Biol Ther 2022; 22: 717-34.

[7] Ali AS, Hayes MC, Birch B, Dudderidge T and Somani BK. Health related quality of life (HRQoL) after cystectomy: comparison between orthotopic neobladder and ileal conduit diversion. Eur J Surg Oncol 2015; 41: 295-9.

[8] Månsson A, Davidsson T, Hunt S and Månsson W. The quality of life in men after radical cystectomy with a continent cutaneous diversion or orthotopic bladder substitution: is there a difference? BJU Int 2002; 90: 386-90.

[9] Matsuda T, Aptel I, Exbrayat C and Grosclaude P. Determinants of quality of life of bladder cancer survivors five years after treatment in France. Int J Urol 2003; 10: 423-9.

[10] VAlastyan S and Weinberg RA. Tumor metastasis: molecular insights and evolving paradigms. Cell 2011; 147: 275-92.
[11] Shah S, Brock EJ, Ji K and Mattingly RR. Ras and Rap1: a tale of two GTPases. Semin Cancer Biol 2019; 54: 29-39.
[12] Zhao F, Vakhrusheva O, Markowitsch SD, Slade KS, Tsaur I, Cinatl J Jr, Michaelis M, Efferth T, Haferkamp A and Juengel E. Artesunate impairs growth in cisplatin-resistant bladder cancer cells by cell cycle arrest, apoptosis and autophagy induction. Cells 2020; 9: 2643.
[13] Kong N, Chen X, Feng J, Duan T, Liu S, Sun X, Chen P, Pan T, Yan L, Jin T, Xiang Y, Gao Q, Wen C, Ma W, Liu W, Zhang M, Yang Z, Wang W, Zhang R, Chen B, Xie T, Sui X and Tao W. Baicalin induces ferroptosis in bladder cancer cells by downregulating FTH1. Acta Pharm Sin B 2021; 11: 4045-54.
[14] Zhou S, Fan X, Du X, Liu S, Sun H and Zhang Y. Effect of traditional Chinese medicine combined with bladder perfusion with hydroxycamptothecin on color ultrasound and clinical efficacy in patients with bladder cancer surgery. Evid Based Complement Alternat Med 2021; 2021: 7178414.
[15] Wang Y, Zhou X, Wei S, Wang G and Xi J. Current status and future challenges in extraction, purification and identification of Cepharanthine (a potential drug against COVID-19). Sep Purif Technol 2023; 309: 123038.
[16] Zhao J, Piao X, Wu Y, Liang S, Han F, Liang Q, Shao S and Zhao D. Cepharanthine attenuates cerebral ischemia/reperfusion injury by reducing NLRP3 inflammasome-induced inflammation and oxidative stress via inhibiting 12/15-LOX signaling. Biomed Pharmacother 2020; 127: 110151.
[17] Zhang S, Huang W, Ren L, Ju X, Gong M, Rao J, Sun L, Li P, Ding Q, Wang J and Zhang QC. Comparison of viral RNA-host protein interactomes across pathogenic RNA viruses informs rapid antiviral drug discovery for SARS-CoV-2. Cell Res 2022; 32: 9-23.
[18] Feng F, Pan L, Wu J, Li L, Xu H, Yang L, Xu K and Wang C. Cepharanthine inhibits hepatocellular carcinoma cell growth and proliferation by regulating amino acid metabolism and suppresses tumorigenesis in vivo. Int J Biol Sci 2021; 17: 4340-52.
[19] Xu W, Wang X, Tu Y, Masaki H, Tanaka S, Onda K, Sugiyama K, Yamada H and Hirano T. Tetrandrine and cepharanthine induce apoptosis through caspase cascade regulation, cell cycle arrest, MAPK activation and PI3K/Akt/mTOR signal modification in glucocorticoid resistant human leukemia Jurkat T cells. Chem Biol Interact 2019; 310: 108726.
[20] Liu Y, Tang Q, Rao Z, Fang Y, Jiang X, Liu W, Luan F and Zeng N. Inhibition of herpes simplex virus 1 by cepharanthine via promoting cellular autophagy through up-regulation of STING/TBK1/P62 pathway. Antiviral Res 2021; 193: 105143.
[21] Chen G, Li J, Liu H, Zhou H, Liu M, Liang D, Meng Z, Gan H, Wu Z, Zhu X, Han P, Liu T, Gu R, Liu S and Dou G. Cepharanthine ameliorates pulmonary fibrosis by inhibiting the NF-κB/NLRP3 pathway, fibroblast-to-myofibroblast transition and inflammation. Molecules 2023; 28: 753.
[22] Liu K, Hong B, Wang S, Lou F, You Y, Hu R, Shafqat A, Fan H and Tong Y. Pharmacological activity of cepharanthine. Molecules 2023; 28: 5019.
[23] Enokida H, Gotanda T, Oku S, Imazono Y, Kubo H, Hanada T, Suzuki S, Inomata K, Kishiye T, Tahara Y, Nishiyama K and Nakagawa M. Reversal of P-glycoprotein-mediated paclitaxel resistance by new synthetic isoprenoids in human bladder cancer cell line. Jpn J Cancer Res 2002; 93: 1037-46.
[24] Hirai M, Tanaka K, Shimizu T, Tanigawara Y, Yasuhara M, Hori R, Kakehi Y, Yoshida O, Ueda K, Komano T, et al. Cepharanthin, a multidrug resistant modifier, is a substrate for P-glycoprotein. J Pharmacol Exp Ther 1995; 275: 73-8.
[25] Lee EH, Chung JW, Sung E, Yoon BH, Jeon M, Park S, Chun SY, Lee JN, Kim BS, Kim HT, Kim TH, Choi SH, Yoo ES, Kwon TG, Kang HW, Kim WJ, Yun SJ, Lee S and Ha YS. Anti-metastatic effect of pyruvate dehydrogenase kinase 4 inhibition in bladder cancer via the ERK, SRC, and JNK pathways. Int J Mol Sci 2022; 23: 13240.
[26] Kaufman DS, Shipley WU and Feldman AS. Bladder cancer. Lancet 2009; 374: 239-49.
[27] Gao S, Li X, Ding X, Qi W and Yang Q. Cepharanthine induces autophagy, apoptosis and cell cycle arrest in breast cancer cells. Cell Physiol Biochem 2017; 41: 1633-48.
[28] Li G, Qiao K, Xu X and Wang C. Cepharanthine regulates autophagy via activating the p38 signaling pathway in lung adenocarcinoma cells. Anticancer Agents Med Chem 2022; 22: 1523-9.
[29] Caron E. Cellular functions of the Rap1 GTP-binding protein: a pattern emerges. J Cell Sci 2003; 116: 435-40.
[30] Kitayama H, Sugimoto Y, Matsuzaki T, Ikawa Y and Noda M. A ras-related gene with transformation suppressor activity. Cell 1989; 56: 77-84.
[31] Li H, Liang J, Wang J, Han J, Li S, Huang K and Liu C. Mex3a promotes oncogenesis through the RAP1/MAPK signaling pathway in colorec-

tal cancer and is inhibited by hsa-miR-6887-3p. Cancer Commun (Lond) 2021; 41: 472-91.
[32] Ma XL, Shen MN, Hu B, Wang BL, Yang WJ, Lv LH, Wang H, Zhou Y, Jin AL, Sun YF, Zhang CY, Qiu SJ, Pan BS, Zhou J, Fan J, Yang XR and Guo W. CD73 promotes hepatocellular carcinoma progression and metastasis via activating PI3K/AKT signaling by inducing Rap1-mediated membrane localization of P110β and predicts poor prognosis. J Hematol Oncol 2019; 12: 37.
[33] Kumar N, Prasad P, Jash E, Saini M, Husain A, Goldman A and Sehrawat S. Insights into exchange factor directly activated by cAMP (EPAC) as potential target for cancer treatment. Mol Cell Biochem 2018; 447: 77-92.
[34] Yang H, Xue W, Ding C, Wang C, Xu B, Chen S, Zha B, Sun Y, Zhu H, Zhang J and Dong L. Vitexin mitigates myocardial ischemia/reperfusion injury in rats by regulating mitochondrial dysfunction via Epac1-Rap1 signaling. Oxid Med Cell Longev 2021; 2021: 9921982.
[35] Rodríguez-Blázquez A, Carabias A, Morán-Vaquero A, de Cima S, Luque-Ortega JR, Alfonso C, Schuck P, Manso JA, Macedo-Ribeiro S, Guerrero C and de Pereda JM. Crk proteins activate the Rap1 guanine nucleotide exchange factor C3G by segregated adaptor-dependent and -independent mechanisms. Cell Commun Signal 2023; 21: 30.
[36] Li QQ, Hsu I, Sanford T, Railkar R, Balaji N, Sourbier C, Vocke C, Balaji KC and Agarwal PK. Protein kinase D inhibitor CRT0066101 suppresses bladder cancer growth in vitro and xenografts via blockade of the cell cycle at G2/M. Cell Mol Life Sci 2018; 75: 939-63.
[37] Medeiros RB, Dickey DM, Chung H, Quale AC, Nagarajan LR, Billadeau DD and Shimizu Y. Protein kinase D1 and the beta 1 integrin cytoplasmic domain control beta 1 integrin function via regulation of Rap1 activation. Immunity 2005; 23: 213-26.
[38] Woods AJ, White DP, Caswell PT and Norman JC. PKD1/PKCmu promotes alphavbeta3 integrin recycling and delivery to nascent focal adhesions. EMBO J 2004; 23: 2531-43.
[39] Wang JF, Chen YY, Zhang SW, Zhao K, Qiu Y, Wang Y, Wang JC, Yu Z, Li BP, Wang Z and Chen JQ. ITGA5 promotes tumor progression through the activation of the FAK/AKT signaling pathway in human gastric cancer. Oxid Med Cell Longev 2022; 2022: 8611306.
[40] Earl J, Rico D, Carrillo-De-Santa-Pau E, Rodríguez-Santiago B, Méndez-Pertuz M, Auer H, Gómez G, Grossman HB, Pisano DG, Schulz WA, Pérez-Jurado LA, Carrato A, Theodorescu D, Chanock S, Valencia A and Real FX. The UBC-40 urothelial bladder cancer cell line index: a genomic resource for functional studies. BMC Genomics 2015; 16: 403.
[41] Loggenberg SR, Twilley D, De Canha MN, Meyer D, Mabena EC and Lall N. Evaluation of wound healing and antibacterial potential of *Greyia radlkoferi* Szyszyl. Ethanolic leaf extract. Front Pharmacol 2022; 13: 806285.
[42] Pathak NN, Lingaraju MC, Balaganur V, Kant V, More AS, Kumar D, Kumar D and Tandan SK. Anti-inflammatory and chondroprotective effects of atorvastatin in a cartilage explant model of osteoarthritis. Inflamm Res 2015; 64: 161-9.
[43] Qi W, Ding D and Salvi RJ. Cytotoxic effects of dimethyl sulphoxide (DMSO) on cochlear organotypic cultures. Hear Res 2008; 236: 52-60.
[44] Che YL, Luo SJ, Li G, Cheng M, Gao YM, Li XM, Dai JM, He H, Wang J, Peng HJ, Zhang Y, Li WY, Wang H, Liu B and Linghu H. The C3G/Rap1 pathway promotes secretion of MMP-2 and MMP-9 and is involved in serous ovarian cancer metastasis. Cancer Lett 2015; 359: 241-9.
[45] Ichikawa H, Itsumi M, Kajioka S, Maki T, Lee K, Tomita M and Yamaoka S. Overexpression of exchange protein directly activated by cAMP-1 (EPAC1) attenuates bladder cancer cell migration. Biochem Biophys Res Commun 2018; 495: 64-70.
[46] Lyle KS, Raaijmakers JH, Bruinsma W, Bos JL and de Rooij J. cAMP-induced Epac-Rap activation inhibits epithelial cell migration by modulating focal adhesion and leading edge dynamics. Cell Signal 2008; 20: 1104-16.
[47] Zhu Z, Xu L, Wan Y, Zhou J, Fu D, Chao H, Bao K and Zeng T. Inhibition of E-cadherin expression by lnc-RNA H19 to facilitate bladder cancer metastasis. Cancer Biomark 2018; 22: 275-81.
[48] Palao N, Sequera C, Cuesta ÁM, Baquero C, Bragado P, Gutierrez-Uzquiza A, Sánchez A, Guerrero C and Porras A. C3G down-regulation enhances pro-migratory and stemness properties of oval cells by promoting an epithelial-mesenchymal-like process. Int J Biol Sci 2022; 18: 5873-84.
[49] Asuri S, Yan J, Paranavitana NC and Quilliam LA. E-cadherin dis-engagement activates the Rap1 GTPase. J Cell Biochem 2008; 105: 1027-37.